On Energy Efficiency of Prioritized IoT Systems: KTH Technical Report

†Abdulrahman Alabbasi, ‡Basem Shihada, and †Cicek Cavdar
† Royal Institute of Technology (KTH) Email: {alabbasi, cavdar}@kth.se ‡ King Abdullah University of Science and Technology (KAUST) Email: basem.shihada@kaust.edu.sa

***Abstract*—The inevitable deployment of 5G and the Internet-of-Things (IoT) sheds the light on the importance of the energy efficiency performance of Device-to-Device (DD) communication systems. In this work, we address a potential IoT application, where different prioritized Device-to-Device system (DDS), i.e., Low-Priority (LP) and High-Priority (HP) systems, co-exist and share the spectrum. We maximize the energy efficiency of each system by proposing two schemes. The first scheme optimizes the individual transmission power and the spatial density of each system. The second scheme optimizes the transmission power ratio of both systems and the spatial density of each one. Unique structures of the addressed problems have been verified. We construct and solve a multi-objective optimization problem to maximize both HP and LP energy efficiency performance. Numerical results are presented to evaluate the system performance.**

***Index Terms*—Spectrum sharing, Energy efficiency, Resource allocation, Stochastic geometry, Device-to-Device,**

I. Introduction

High throughput data communication and reliable (long life-time and large capacity) sensor networks are major components that lead to the realization of 5G and IoT. These emerging technologies lead to significant power consumption requirements. Therefore, energy measurement metrics are essential for realizing future technologies and guaranteeing a certain energy efficiency performance. Researchers have been thoroughly investigating the greenness of communication networks. Variety of energy efficiency (EE) metrics have been proposed based on different factors and several communication layers, e.g., routing, media access control (MAC), and physical (PHY) layers, and cross layer design, [1]–[3]. A recently developed tool, called stochastic geometry, has shown solid techniques to provide tractable expressions for spatially random wireless systems[4], while including the impact of several layers parameters.

Stochastic geometric tools have been utilized to capture the spatial randomness of wireless network's nodes [4]. Several works have tackled the outage probability and spatial capacity of communication networks using stochastic geometric tools [4]–[9]. However, working on utilizing this tool in improving the energy efficiency is still an open research problem. The authors of [10] have tackled the energy efficiency performance of a heterogeneous network. Fairness of the sub-channel allocation have also been addressed. On the other hand, authors of [11] have addressed the EE maximization of several sharing systems from a game theory perspective. They considered non-cooperative game between different systems, with and without incorporating pricing to the power control game. In a cellular system, authors of [12] have modeled a system that contains both macro basestations (MBSs) and femto-cell access points (FAPs) and their associated user equipments (UEs) as two independent Poisson point processs (PPPs). They assumed that there is not interference between different systems, unlike our work which considered the inter/intra interference. They maximized EE, derived throughput per power, with respect to (w.r.t.) sub-channels allocation, while taking the impact of different diversity schemes. The authors of [13] modeled the two-tier cellular system's components, i.e., MBSs, small-cell access points (SAPs), and UEs as independent PPPs. They analyzed the data rate associated with different communication scenarios, i.e., MBS-to-UE, SAP-to-UE, and MBS-to-SAP. They obtained the EE by dividing the analyzed data rate by the associated system's power.

In this work, we consider a network model where two multiple users systems, i.e., HP system and LP system, co-exist in the same area. We capture the spatial randomness of the nodes under both systems by utilizing the stochastic geometric framework. The targeted performance metric of all systems is the energy efficiency, defined as, the transmission capacity (successful transmissions per unit area) to power ratio. We enforce outage probability constraint on Low-Priority user (LPU) transmission to guarantee minimum High-Priority system (HPS)'s quality of service (QoS).

Our contribution is as follows. We maximize the individual EE of both LPU and High-Priority user (HPU) systems. This maximization is conducted via proposing two schemes, i.e., scheme 1 and scheme 2. Optimal transmission power and spatial density of each system are derived in scheme 1. The corresponding strict pseudo-concave and quasi-concave structures of the problem are verified in scheme 1. Whereas, Optimal transmission power ratio of both systems and spatial density of each system are derived in scheme 2. In this scheme, the joint strict pseudo-concave and quasi-concave structures of the associated problem have been verified. We also show the distinctions between both schemes. We then construct an over all multi-objective EE of both LPU and HPU systems. Several multi-objective combination methodologies are used to solve the problem. However, because of the page limitation in this work, we only introduce the Linear-Scalarizing method (LSM). In this approach, we maximize a linear combination of LPU's EE and HPU's EE systems with respect to LPU's and HPU's transmission power and spatial density. The global joint optimal solution set is obtained via verifying a unique structure fo the joint optimization problem and proposing an alternating algorithm, while satisfying the necessary and

This work was conducted at Monash University, Melbourne. The authors would like to thank Prof. Jamie Evans for his support.

sufficient conditions.

In the following, we show the distinction points between our proposed model and solution and the existing ones. Unlike our contribution, the work of [10] did not derive the optimal power allocation of the associated problem. Also, the authors of [11] did not provide analytical results to both nodes densities and transmission power. They also did not combine EE of several sharing systems. The problem model of [12], [13] is based on a master slave communication system, unlike our prioritized DD in-band sharing system. Also, different optimization variables and solution methodolgies are considered in The work in [13] differs from ours in several points. In our model, we consider communication between pairs of DD nodes, that belongs to different systems with distinct priorities, not necessarily master-slave network topology, as in cellular system. We also do not ignore the interference of different communication pairs. The formulation of EE metric in [13], [14] is also different from our model, where we consider distinct optimization variables and combination methods, to jointly maximize the EE of both sharing systems.

II. System Model and Transmission Capacity

Targeting the energy efficiency of spectrum sharing networks requires obtaining each system's capacity. In this section, we describe the network's system model and the transmission capacity of each system in the network.

A. Spectrum Sharing Network Model

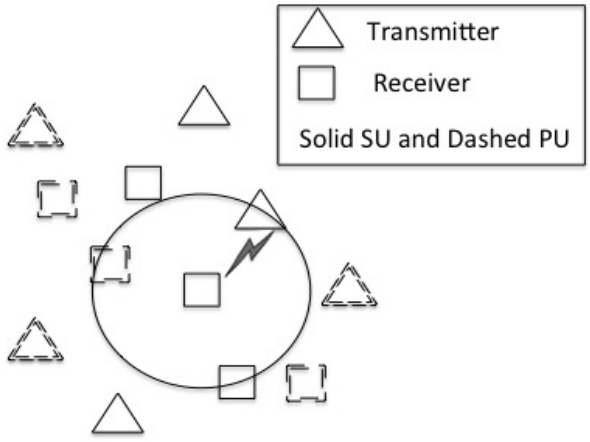

Fig. 1. System model of multiple LP and HP users that coexist and share the spectrum in a certain area.

Figure 1 describes the model of two coexisting networks. The nodes in Fig. 1 represent both LP network's transmitters and receivers (represented by solid line) and HP network's transmitters and receivers (represented by dashed line). The set of all transmitter nodes, i.e., $\{s,p\} \in \Phi$, follows PPP, where the nodes uniformly distributed in the captured area. This distribution is well accepted in the literature because of the randomness of the nodes locations, i.e., this distribution represents the worst-case scenarios among other distributions. For instance, in [15], authors assumed models where the transmitters have to satisfy a minimum guard zone distance toward the potential receivers. The mean of the PPP distributed nodes is λ_q, where $q \in \{s,p\}$. This is interpreted as the average number of nodes in a unit area is equal to λ_q. Since different receiving nodes have similar received signal statistics, we therefore conduct the analysis on a receiving node at the origin of the map. The interfering nodes follow a marked Poisson point process (MPPP), i.e., transmitting nodes of a system q are expressed as $\Xi_q = \{(\mathcal{X}_{qj}, h_{qj})\}$. The location of the transmitter is noted as $\mathcal{X}_{qj}$ and the channel between the transmitter and the receiving node (at the origin) is h_{qj}. This channel follows a Rayleigh distribution with a unity mean and its modulus squared is expressed as $|h_{qj}|^2 = \gamma_{qj}$. We also assume that all the transmission nodes in each system transmit with the same adaptive power, i.e., P_q for $q \in \{s,p\}$. The received power at the desired receiver is expressed as $|x_q|^{-\alpha} P_q \gamma_{qj}$ for $q \in \Phi$, where $|x_q|$ is the distance to the receiving node at the origin and α is the pathloss exponent. Note that we omit the j of the studied receiving node since it is at the origin.

B. Success Probability and Transmission Capacity

In this section, we define both the successful transmission probability of each sharing network and the associated transmission capacity.

In order to express the targeted system's signal to noise and interference ratio (SINR), say it is system t, we consider all interferences from the same system, t, and the other system, q. The corresponding SINR of the targeted system is expressed as follows,

$$\mathrm{SINR}_t = \frac{|x_t|^{-\alpha} P_t \gamma_{ti}}{\sum_{q\in\Phi} \sum_{x_q \in \Xi_q} |x_q|^{-\alpha} P_q \gamma_q + \mathcal{N}_0}. \tag{1}$$

We ignore the effect of the thermal noise, since we assume the interference from all the nodes has larger effect on the desired signal compared to the thermal noise. Therefore, in our analysis, we consider the targeted signal to interference ratio (SIR). Hence, the successful transmission probability is defined as follows,

$$\mathbb{P}_t = \Pr\Big\{ \Theta_t \geq \theta_t \Big\} = \Pr\Big\{ \underbrace{\frac{|x_t|^{-\alpha} P_t \gamma_t}{\sum\limits_{q\in\Phi} \sum\limits_{x_q\in\Xi_q} |x_q|^{-\alpha} P_q \gamma_q}}_{\mathcal{I}_t} \geq \theta_t \Big\}, \tag{2}$$

Note that the interference is a sum of measurable functions of a MPPP. It follows that after applying several known techniques (i.e., Laplace transformation, Campbell's Theorem, random variable conditioning, and change of variable) on (2), the successful transmission probability expression of the LP system is found as follows [4],

$$\mathbb{P}_l = \exp\left(-\eta_l' \left(\lambda_l + \lambda_h \left(\frac{P_h}{P_l} \right)^{\frac{2}{\alpha}} \right) \right), \tag{3}$$

where $\eta_t' = \pi R_t^2 \theta_t^{\frac{2}{\alpha}}$. The successful transmission probability of the HP system is found in similar lines to that of the LP system while switching the sub-script of the parameter from x_l to x_h, where x is any symbol that is used interchangeably for both LP and HP systems.

In order to study the energy efficiency, the associated transmission capacity of each system in the sharing area must be obtained. The corresponding LP's transmission capacity is expressed as follows,

$$\mathcal{T}_l = \lambda_l \exp\left(-\eta_l'\left(\lambda_l + \lambda_h\left(\frac{P_h}{P_l}\right)^{\frac{2}{\alpha}}\right)\right), \tag{4}$$

The HP's transmission capacity is also find in similar lines with (4) while changing the sub-script because of the symmetry between both expressions.

III. Achievable Energy Efficiency of LPU and HPU

In this section, we formulate the energy efficiency metric of LPU's network and derive the optimal solution, i.e., transmission power and spatial density. Following similar steps, we derive the optimal solution of the energy efficiency performance of HPU network.

The energy efficiency of LPU's network is defined as the ratio of the transmission capacity to power, i.e.,

$$\mathcal{E}_l(P_l, \lambda_l, P_h, \lambda_h) = \lambda_l \frac{\exp\left(-\eta_l'\left(\lambda_l + \lambda_h\left(\frac{P_h}{P_l}\right)^{\frac{2}{\alpha}}\right)\right)}{(k_t P_l + k_c)}, \tag{5}$$

where k_c and k_t are assigned parameters which correspond to the circuit power of the radio device and the power amplifier constant power consumption.

The energy efficiency problem of LPU's system maximizes LPU's EE metric subject to maintaining a certain LPU's outage probability and a certain HPU's outage probability. The targeted problem is expressed as follows,

$$\max \quad \lambda_l \frac{\exp\left(-\eta_l'\left(\lambda_l + \lambda_h\left(\frac{P_h}{P_l}\right)^{\frac{2}{\alpha}}\right)\right)}{(k_t P_l + k_c)} \tag{6a}$$

$$\text{s.t.} \quad \mathfrak{C}_1\colon 1 - \exp\left(-\eta_l'\left(\lambda_l + \lambda_h\left(\frac{P_h}{P_l}\right)^{\frac{2}{\alpha}}\right)\right) \leq \epsilon_l \tag{6b}$$

$$\mathfrak{C}_2\colon 1 - \exp\left(-\eta_h'\left(\lambda_h + \lambda_l\left(\frac{P_l}{P_h}\right)^{\frac{2}{\alpha}}\right)\right) \leq \epsilon_h \tag{6c}$$

We propose two schemes to solve problem (6). The main difference between the two schemes is the definition of the optimization variables. In scheme 1, we maximize problem (6) by optimizing LPU's transmission power and LPU's spatial density. In scheme 2, we maximize problem (6) by jointly optimizing the transmission power ratio, i.e., $\zeta_n = \frac{P_h}{P_l}$, and LPU's spatial density.

1) Scheme 1: In this scheme, we optimize LPU's transmission power, P_l, and LPU's spatial density, λ_l.

We begin by converting the probabilistic constraints $\mathfrak{C}_1$ and $\mathfrak{C}_2$ into an instantaneous constraint. These constraints acts as boundaries for each of the optimization variables, i.e., P_l and λ_l. Constraint $\mathfrak{C}_1$ upper bounds the transmission power as follows,

$$P_l \leq \left[\frac{\log(1-\epsilon_h)^{-1}}{\lambda_l \eta_h'} - \frac{\lambda_h}{\lambda_l}\right]^{\frac{\alpha}{2}} P_h = P_s^+, \tag{7}$$

whereas constraint $\mathfrak{C}_2$ lower bounds LPU's transmission power as follows,

$$P_l \geq \left[\frac{\log(1-\epsilon_l)^{-1}}{\lambda_h \eta_l'} - \frac{\lambda_l}{\lambda_h}\right]^{\frac{-\alpha}{2}} P_h = P_s^-. \tag{8}$$

Maximizing problem (6) with respect to LPU's transmission power is difficult to solve by conventional method. That is due to the fractional, exponential, and geometrical nature of parameter P_l in (6a). In order to find the optimal P_l which maximizes (6) we follow several steps as follows. We apply a geometric optimization technique, change of variable, on parameter P_l such that, $P_n = (P_l)^{\frac{2}{\alpha}}$ and $P_l = (P_n)^{\frac{\alpha}{2}}$. Since the change of variable function is monotone over the range of $P_l \geq 0$, we know from [16] that optimizing problem (6) with respect to P_n is equivalent to optimizing it with respect to P_l. We then apply transformation technique to the objective function in (6a), i.e., $\hat{\mathcal{E}}_l = f_0(\mathcal{E}_l)$, where $f_0(\mathcal{E}_l) = \log(\mathcal{E}_l)$. It is proven in [16] that if $f_0(.)$ is $\mathbb{R} \to \mathbb{R}$ and monotonic increasing function, then maximizing $\mathcal{E}_l$ is equivalent to maximizing $\hat{\mathcal{E}}_l = f_0(\mathcal{E}_l)$. It is observed that these conditions are satisfied by the logarithmic function. Taking into account that both constraints $\mathfrak{C}_1$ and $\mathfrak{C}_2$ are peak constraints on P_l, thus we apply them after obtaining the optimal P_l. Problem (6) is transformed into the following problem,

$$\max_{(P_s^-)^{\frac{2}{\alpha}} \leq P_n \leq (P_s^+)^{\frac{2}{\alpha}}} \log\left[\frac{\lambda_l \exp\left(-\eta_l'\left(\lambda_l + \lambda_h \frac{P_h^{\frac{2}{\alpha}}}{P_n}\right)\right)}{k_t P_n^{\frac{\alpha}{2}}}\right]. \tag{9}$$

The solution of problem (9) is summarized in the following lemma.

Lemma 1. *The optimal LPU's transmission power that maximizes problem (9) is expressed as follows,*

$$\hat{P}_l = \min\left\{\max\{P_l^*, P_s^-\}, P_s^+\right\}, \tag{10}$$

where P_l^* is expressed as follows,

$$P_l^* = \left(\frac{2\eta_l' \lambda_h}{\alpha}\right)^{\frac{\alpha}{2}} P_h. \tag{11}$$

Proof. The proof is given in Appendix A. □

It is observed that the optimal LPU's transmission power increases with the increase of HPU's transmission power and HPU's spatial density.

We now find the optimal LPU's spatial density which maximizes problem (6). We begin by transforming constraints $\mathfrak{C}_1$ and $\mathfrak{C}_2$ as upper bounds to the spatial density. Let us note the total upper bound as follows,

$$\lambda_s^+ = \min\left(\lambda_{s1}^+, \lambda_{s2}^+\right), \tag{12}$$

where

$$\lambda_{s1}^+ = \left[\frac{\log(1-\epsilon_h)^{-1}}{\eta_h'} - \lambda_h\right]\left(\frac{P_h}{P_l}\right)^{\frac{2}{\alpha}}, \tag{13}$$

and

$$\lambda_{s2}^{+}=\left[\frac{\log\left(1-\epsilon_l\right)^{-1}}{\eta_l'}-\lambda_h\left(\frac{P_h}{P_l}\right)^{\frac{2}{\alpha}}\right]. \tag{14}$$

We then rewrite problem (6) as follows,

$$\max_{\lambda_l\leq\lambda_s^{+}}\frac{\lambda_l\exp\left(-\eta_l'\left(\lambda_l+\lambda_h\left(\frac{P_h}{P_l}\right)^{\frac{2}{\alpha}}\right)\right)}{k_tP_l}. \tag{15}$$

The solution of problem (15) is summarized in the following lemma.

Lemma 2. *The optimal LPU's spatial density that maximizes problem (15) is expressed as follows,*

$$\hat{\lambda_l}=\min\left\{\lambda_s^{+},\frac{1}{\eta_l'}\right\}. \tag{16}$$

Proof. The proof is given in Appendix B □

Note that the optimal LPU's spatial density decreases with the increase of the distance between nodes and the increase of the SIR threshold.

Note that in order to get the optimal expressions of transmission power and nodes spatial density for the HP system, we face two choices. One is to protect the LP users transmission via similar constraint to that in $\mathfrak{C}_2$ in (6) but from HP transmission perspective. In this case, both the optimal power and user density, are found in similar lines with the ones for LP system while changing the sub-script. The other choice is not to protect the LP's transmission. Hence, the upper bound on the optimal HP's transmission power is discarded. Also, one of the two upper bounds on the HPU's spatial density is discarded, as the HP system does not care about the LP system performance. Otherwise, all derivation steps are similar to that of the LP system parameters.

2) Scheme 2: In this scheme, we maximize problem (6) by jointly optimizing the transmission power ratio, i.e., $\zeta_n=\frac{P_h}{P_l}$, and LPU's spatial density, i.e., λ_l. The main advantage of this scheme over scheme 1 is that the joint optimal solution is guaranteed without the necessity to use an alternating iterative algorithm.

After substituting $\zeta_s=\left(\frac{P_h}{P_l}\right)^{\frac{2}{\alpha}}$ in problem (6), the targeted optimization problem is rewritten as follows,

$$\max_{\zeta_s,\lambda_l}\quad \lambda_l\frac{\exp\left(-\eta_l'\left(\lambda_l+\lambda_h\zeta_s\right)\right)}{\left(k_tP_h\zeta_s^{\frac{-\alpha}{2}}\right)} \tag{17a}$$

$$\text{s.t.}\quad \mathfrak{C}_1\text{: }\lambda_l+\lambda_h\zeta_s+\frac{1}{\eta_l'}\log\left(1-\epsilon_l\right)\leq 0 \tag{17b}$$

$$\mathfrak{C}_2\text{: }\lambda_l+\zeta_s\left(\lambda_h+\frac{1}{\eta_h'}\log\left(1-\epsilon_h\right)\right)\leq 0 \tag{17c}$$

The solution of problem (17) is summarized in the following theorem.

Theorem 1. *The global joint optimal solution set of problem (17) is obtained as follows.*

The optimal transmission power ratio is expressed as,

$$\hat{\zeta_s}=\frac{2}{\alpha}\left[\lambda_h\left(\eta_s'+\lambda_1+\lambda_2\right)+\frac{\lambda_2}{\eta_p'}\log(1-\epsilon_p)\right]^{-1}. \tag{18}$$

The optimal LPU's spatial density is expressed as,

$$\hat{\lambda_l}=\frac{1}{\eta_s'+\lambda_1+\lambda_2}. \tag{19}$$

The Lagrangian multipliers λ_1 and λ_2 are obtained by solving the Karush-Kuhn-Tucker (KKT) conditions associated with $\mathfrak{C}_1$ and $\mathfrak{C}_2$, respectively.

Proof. The proof of Theorem 1 is given in Appendix C. □

Remark 1. It is interesting to note that both solutions of problem (6), under scheme 1, and problem (17), under scheme 2, are equivalent. Note that under inactive constraints, i.e., $\lambda_1=0$ and $\lambda_2=0$, the LPU's transmission power, obtained from the optimal ζ_s in (18), is equal to P_l^{*} in (11). Similarly, under inactive constraints we note that $\hat{\lambda_l}$ in (19) is equivalent to that in (16).

To maximize HPU's energy efficiency utilizing scheme 2, we use similar analogue to that of scheme 1 in the HPU solution part.

IV. Linearly Combined EE LPU and HPU Systems

In this section, we maximize a weighted sum of $\mathcal{E}_l$ and $\mathcal{E}_h$ with respect to transmission power of both LPU and HPU systems in addition to the spatial density of both LPU and HPU system. This problem is extremely complicated to solve, because the joint concavity or quasi-concavity structure of the objective function with respect to all optimization variables cannot be verified. Therefore, we solve this problem by individually maximizing the problem with respect to each optimization variable. We then find the optimal expression for each variable. Finally, we propose an iterative algorithm, which utilizes the individual optimality of each variable to guarantee a global joint optimal solution of the problem.

The formulation of the weighted sum total energy efficiency metric problem is expressed as follows,

$$\max\quad \mathcal{E}_{TS}=\alpha_l\mathcal{E}_l\left(P_l,P_h,\lambda_l,\lambda_h\right)+\alpha_h\mathcal{E}_h\left(P_l,P_h,\lambda_l,\lambda_h\right) \tag{20a}$$

$$\text{s.t.}\quad \mathfrak{C}_1;\quad \mathfrak{C}_2; \tag{20b}$$

where α_s and α_p are the weighting parameters of each metric. It is difficult to find a joint structure, i.e., concavity, pseudo-concavity, or quasi-concavity, of problem (20) with respect to to all optimization variables. Therefore, we begin our solution by maximizing problem (20) with respect to each variable separately, i.e., P_l, λ_l, P_h, and λ_h, respectively.

The optimal P_l which maximizes problem (20) cannot be obtained in a similar way to the optimal P_l which maximizes (6). This is due to the existence of P_l in the exponential term of $\mathcal{E}_h$. Furthermore, it is not possible to, analytically, find the zeros of the first derivative of Lagrangian function to solve (20) with respect to P_l. That is because there is a weighted sum of exponential terms and each one includes a different function of P_l. For further illustration, note that the exponential term of $\mathcal{E}_l$ is expressed as $\eta_l'\lambda_h\left(\frac{P_h}{P_l}\right)^{\frac{2}{\alpha}}$ whereas the exponential term of $\mathcal{E}_h$ is expressed as $\eta_h'\lambda_l\left(\frac{P_l}{P_h}\right)^{\frac{2}{\alpha}}$. To overcome this problem, we introduce a new variable, i.e., P_{sp}. This variable replaces P_l

in HPU's $\mathcal{E}_h$ term, i.e., $\mathcal{E}_h = \frac{\lambda_h \exp\left(-\eta_h'\left(\lambda_h+\lambda_l\left(\frac{P_{sp}}{P_h}\right)^{\frac{2}{\alpha}}\right)\right)}{\left(k_t P_h + k_c\right)}$. A new constraint must be added to link both variables, i.e., $P_l = P_{sp}$. We then apply the change of variables to both P_l and P_{sp}, such that $P_n = P_l^{\frac{2}{\alpha}}$ and $P_{np} = P_{sp}^{\frac{2}{\alpha}}$. The maximization problem of (20) is rewritten as follows,

$$\max_{(P_s^-)^{\frac{2}{\alpha}} \leq \{P_n, P_{np}\} \leq (P_s^+)^{\frac{2}{\alpha}}} \quad \alpha_l \mathcal{E}_l\left(P_n\right) + \alpha_h \mathcal{E}_h\left(P_{np}\right) \tag{21a}$$

$$\text{s.t.} \quad P_n = P_{np} \tag{21b}$$

Remark 2. Note that the second term of (21a) is constant with respect to P_n, i.e., $\frac{\alpha_h \lambda_h \exp\left(-\eta_h'\left(\lambda_h+\lambda_l \frac{P_{np}}{P_h^{\frac{2}{\alpha}}}\right)\right)}{\left(k_t P_h + k_c\right)}$ is not a function of P_n. Whereas the first term in (21a) is constant with respect to P_{np}, i.e., $\frac{\lambda_l \exp\left(-\eta_l'\left(\lambda_l+\lambda_h \frac{P_h^{\frac{2}{\alpha}}}{P_n}\right)\right)}{k_t P_n^{\frac{\alpha}{2}} + k_c}$ is not a function of P_{np}.

Utilizing Remark 2 and the geometric optimization techniques, which are used in Sec. III, we obtain the optimal value of P_l in the following proposition.

Proposition 1. *The optimal value of P_n that maximizes (20), given P_h and λ_h, is expressed as follows,*

$$\hat{P_n} = \min\{\max\{P_n^o, \left(P_s^-\right)^{\frac{2}{\alpha}}\}, \left(P_s^+\right)^{\frac{2}{\alpha}}\} \tag{22}$$

where

$$P_n^o = \left[\frac{\alpha + \sqrt{\alpha^2 - 16\mu\eta_s'\lambda_h P_h^{\frac{2}{\alpha}}}}{4\mu}\right] \tag{23}$$

P_s^+ and P_s^- are expressed in (7) and (8), respectively. Whereas, the optimal value of P_{np} that maximizes (20), given P_h, λ_l, and λ_h, is expressed as follows,

$$\hat{P_{np}} = \min\{\max\{P_{np}^o, \left(P_s^-\right)^{\frac{2}{\alpha}}\}, \left(P_s^+\right)^{\frac{2}{\alpha}}\} \tag{24}$$

where

$$P_{np}^o = \frac{P_h^{\frac{2}{\alpha}}}{\eta_p'\lambda_l} \log\left[\frac{\eta_p'\lambda_l\lambda_h\alpha_p e^{-\eta_p'\lambda_h}}{\mu k_t P_h^{\frac{2}{\alpha}+1}}\right] \tag{25}$$

The parameter μ, in both (23) and (25), is the Lagrangian multiplier associated with the equality constraint in (21b). The value of μ is obtained by finding the zeros of the following function.

$$g(\mu) = \left[2w\mu - \frac{\mu P_h^{\frac{2}{\alpha}}}{\eta_h'\lambda_l}\log(\mu) - \frac{\alpha}{2}\right]^2 - \frac{\alpha^2}{4} + 4\mu\eta_l'\lambda_h P_h^{\frac{2}{\alpha}} = 0 \tag{26}$$

where $w = \frac{P_h^{\frac{2}{\alpha}}}{\eta_p'\lambda_l}\left[\log\left(\eta_p'\lambda_l\alpha_h\lambda_h e^{-\eta_h'\lambda_h}\right) - \log\left(k_t P_h^{1+\frac{2}{\alpha}}\right)\right]$.

Proof. The proof is given in Appendix D. □

We now solve for the value of λ_l that maximizes problem (20). Utilizing similar geometric optimization techniques that are used in Sec. III and after some algebraic manipulations we find that maximizing problem (20) with respect to λ_l is similar to the following maximization problem.

$$\max_{\lambda_l \leq \lambda_s^+} \log\left(e^{-\eta_l'\lambda_l}\left(a_s\lambda_l + c_s e^{-d_s\lambda_l}\right)\right) \tag{27}$$

where $a_s = \frac{\alpha_l}{k_t P_l}\exp\left(-\eta_l'\lambda_h \frac{P_h^{\frac{2}{\alpha}}}{P_l^{\frac{2}{\alpha}}}\right)$, $c_s = \frac{\alpha_h}{k_t P_h}\exp\left(-\eta_h'\lambda_h\right)$, and $d_s = \eta_h' \frac{P_l^{\frac{2}{\alpha}}}{P_h^{\frac{2}{\alpha}}} - \eta_s'$. The upper bound λ_s^+ is expressed in (12). The solution of problem (27) is summarized in the following proposition.

Proposition 2. *The optimal spatial density of LPU that maximizes (27), given P_h, P_l, and λ_h, is expressed as follows,*

$$\hat{\lambda_l} = \min\{\lambda_l^o, \lambda_s^+\}, \tag{28}$$

where

$$\lambda_l^o = \left[\frac{1}{\eta_l'} + \frac{1}{d_s}W\left[-\frac{c_s d_s(\eta_l' + d_s)}{a_s\eta_l'}\exp\left(-\frac{d_s}{\eta_l'}\right)\right]\right]^+. \tag{29}$$

Proof. The proof is given in Appendix E. □

We optimize HPU's transmission power in similar lines as in optimizing the LPU's parameters. We apply the change of variable to P_h such that $P_u = P_h^{\frac{2}{\alpha}}$. We then introduce a new optimization variable related to the HPU's transmission power, i.e., P_{us} and the corresponding equality constraint $P_{us} = P_u$. The optimal value of P_u which maximizes problem (20) is derived in the following proposition.

Proposition 3. *The optimal value of P_u that maximizes (20), given P_l and λ_l, is expressed as follows,*

$$\hat{P_u} = \min\{\max\{P_u^o, \left(P_p^-\right)^{\frac{2}{\alpha}}\}, \left(P_p^+\right)^{\frac{2}{\alpha}}\} \tag{30}$$

where

$$P_u^o = \left[\frac{\alpha + \sqrt{\alpha^2 - 16\mu_p\eta_p'\lambda_l P_l^{\frac{2}{\alpha}}}}{4\mu_h}\right]^{\frac{\alpha}{2}} \tag{31}$$

and P_p^+ and P_p^- are expressed similar to that in (7) and (8), respectively. Whereas, the optimal value of P_{us} that maximizes (20), given P_l, λ_l, and λ_h, is expressed as follows,

$$\hat{P_{us}} = \min\{\max\{P_{us}^o, \left(P_s^-\right)^{\frac{2}{\alpha}}\}, \left(P_s^+\right)^{\frac{2}{\alpha}}\} \tag{32}$$

where

$$P_{us}^o = \frac{P_l^{\frac{2}{\alpha}}}{\eta_s'\lambda_h} \log\left[\frac{\eta_s'\lambda_h\lambda_l\alpha_s e^{-\eta_s'\lambda_l}}{\mu_p k_t P_l^{\frac{2}{\alpha}+1}}\right] \tag{33}$$

The parameter μ_p is the Lagrangian multiplier associated with the equality constraint similar to that introduced for the LPU's power optimization case, in (21b). The parameter μ_h is obtained by finding the zeros of the following function.

$$g(\mu_p) = \left[2w_p\mu_p - \frac{\mu_p P_l^{\frac{2}{\alpha}}}{\eta_l'\lambda_h}\log(\mu_p) - \frac{\alpha}{2}\right]^2 - \frac{\alpha^2}{4} + 4\mu_p\eta_h'\lambda_l P_l^{\frac{2}{\alpha}} \tag{34}$$

where $w_p = \frac{P_l^{\frac{2}{\alpha}}}{\eta_s'\lambda_h}\left[\log\left(\eta_s'\lambda_h\alpha_l\lambda_l e^{-\eta_l'\lambda_l}\right) - \log\left(k_t P_l^{1+\frac{2}{\alpha}}\right)\right]$.

Proof. The proof is obtained using similar steps to the proof of Proposition 1. □

In the following proposition, we find the value of λ_h which maximizes problem (20).

Proposition 4. *The optimal spatial density of HPU's system that maximizes (20), given P_h, P_l, and λ_l, is expressed as follows,*

$$\hat{\lambda_h} = \min\{\lambda_h^o, \lambda_p^+\} \tag{35}$$

The parameter λ_p^+ is found similar to that in (12). The expression of λ_l^o is obtained as follows,

$$\lambda_h^o = \left[\frac{1}{\eta_h'} + \frac{1}{d_p} W\left[-\frac{c_p d_p(\eta_h' + d_p)}{a_p \eta_h'} \exp\left(-\frac{d_p}{\eta_h'}\right)\right]\right]^+ \tag{36}$$

where $a_p = \frac{\alpha_h}{k_t P_h} \exp\left(-\eta_h' \lambda_l \frac{P_l^{\frac{2}{\alpha}}}{P_h^{\frac{2}{\alpha}}}\right)$, $c_p = \frac{\alpha_l}{k_t P_l} \exp\left(-\eta_l' \lambda_l\right)$, *and* $d_p = \eta_l' \frac{P_h^{\frac{2}{\alpha}}}{P_l^{\frac{2}{\alpha}}} - \eta_p'$.

Proof. The proof is easy to obtain following similar steps as in the proof of Proposition 2. □

After finding the optimal values of $\{P_n, P_{np}, \lambda_l, P_u, P_{us}, \lambda_h\}$ which, individually, maximizes (20), we now introduce an algorithm which enables us to jointly maximize (20). This algorithm utilizes the individual structure of the main problem in (20) with respect to each optimization variables, i.e., no need to verify the joint structure. The proposed algorithm, Algorithm 1, iterates over the previously found optimal values and update them in each iteration to obtain a joint optimal set. The following theorem introduces the joint optimal solution of problem (20).

Theorem 2. *Given a strict quasi-concave structure of problem (20) with respect to each of the optimization variable, the global optimal solution of problem (20) is found through two steps. First, find the optimal variables (P_l, λ_l, P_h, λ_h) as in (22), (28), (30), (35), respectively. Second, update and iterate over these values (P_l, λ_l, P_h, λ_h) using the proposed alternating algorithm in Algorithm 1.*

Proof. The proof is given in Appendix F □

Note that P_{pk}, mentioned at the initialization stage of the algorithm is the maximum allowable transmission power.

V. Numerical Evaluation

In this section, we evaluate the EE performance of the proposed problems, i.e., $\mathcal{E}_l$ (Sec. III) and $\mathcal{E}_{TS}$ (Sec. IV). Note that through out the numerical results we use the following notations. The legend OPL is used to note that this result is associated with optimizing both spatial density and transmission power of the targeted system, whereas, OP or OL are used to note that this result is obtained by optimizing only the transmission power or the spatial density of the targeted system, respectively. The performance measure EE_l represents the LPU's EE as formulated in Sec. III, whereas, EE_TS represents the linear combination of both LPU and HPU systems' EE as formulated in Sec. IV. It is worth noting that under EE_TS scenario, the OPL and OP schemes optimize (in addition to spatial densities) w.r.t. $\zeta = \frac{P_l}{P_h}$ not P_l and P_h, individually. Hence, the denominator of $\mathcal{E}_l$ and $\mathcal{E}_h$ in (20), becomes $P_l = \zeta P_h$ and P_h, respectively, since we assume that the HPS's power is not likely to be changed. The reason behind this substitution is that we find it more numerically stable to optimize w.r.t. to ζ. Note that the unit of EE is successful transmission per watt per unit-area, it could be easily converted to nats per joule per unit area via multiplying the objective function by $\log(1+\theta_s)$.

Algorithm 1: LSM Algorithm

input : η_l', η_h', ϵ_l, ϵ_h, α, α_s, α_p, k_t, P_{pk}, ϵ

Initialize: $\lambda_l^{(0)} = \frac{1}{\eta_s'}$, $\lambda_h^{(0)} = \frac{1}{\eta_h'}$, $P_l^{(0)} = P_{pk}$, $P_h^{(0)} = P_{pk}$, $cond = True$;

$q = 1$

while *cond* **do**

- To find LPU's transmission power, we first solve for μ using (26), given fixed $P_h = P_h^{(q-1)}$, $\lambda_l = \lambda_l^{(q-1)}$, and $\lambda_h = \lambda_h^{(q-1)}$. By finding μ we guarantee that $P_n = P_{np}$. Thus, LPU's power is found as $P_l^{(q)} = \hat{P_n}$, in (22).
- For the values of $P_l = P_l^{(q)}$, $P_h = P_h^{(q-1)}$, and $\lambda_h = \lambda_h^{(q-1)}$, find the LPU's spatial density, i.e., $\lambda_l^{(q)} = \hat{\lambda_l}$, as in (28).
- Given $P_l = P_l^{(q)}$, $\lambda_l = \lambda_l^{(q)}$, and $\lambda_h = \lambda_h^{(q-1)}$, we find the parameter μ_p which guarantee that $P_u = P_{us}$. We then find the HPU's transmission power, i.e., $P_h^{(q)} = \hat{P_u}$, as in (30).
- Find HPU's spatial density, i.e., $\lambda_h^{(q)} = \hat{\lambda_h}$, by substituting $P_l = P_l^{(q)}$, $\lambda_l = \lambda_l^{(q)}$, and $P_h = P_h^{(q)}$ in (35).
- Evaluate $\mathcal{E}_{TS}^{(q)} = \alpha_l \mathcal{E}_l(P_l^{(q)}, \lambda_l^{(q)}, P_h^{(q)}, \lambda_h^{(q)}) + \alpha_h \mathcal{E}_h(P_l^{(q)}, \lambda_l^{(q)}, P_h^{(q)}, \lambda_h^{(q)})$, where
- $\mathcal{E}_l(P_l, \lambda_l, P_h, \lambda_h)$ and $\mathcal{E}_h(P_l, \lambda_l, P_h, \lambda_h)$ are LPS's and HPS's EE, respectively.
- **if** $\left\| \mathcal{E}_{TS}^{(q)} - \mathcal{E}_{TS}^{(q-1)} \right\| < \epsilon$ **then:** $cond = False$
- q = q+1;

end

output: $\{P_l^{(q)}, \lambda_l^{(q)}, P_h^{(q)}, \lambda_h^{(q)}\}$

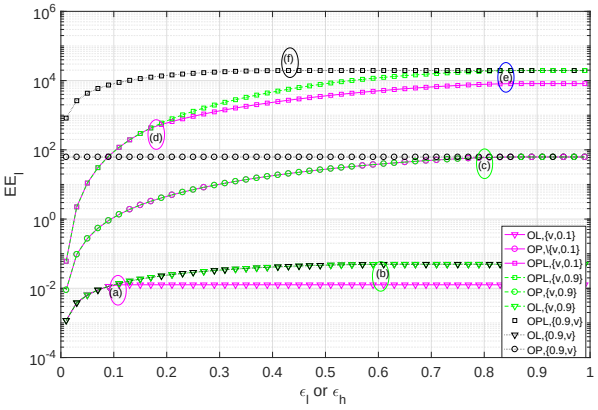

Fig. 2. LPS's EE versus tolerance threshold. Parameters: $P_{l,h}$=25dBm,$\theta_{l,h}$=10.5dB,$R_{l,h}$=2m,k_t=1, $\lambda_{l,h}$=0.5e-4.

Figure 2 evaluates EE, EE_l, against tolerance parameters ϵ_l and ϵ_h, for different schemes (i.e., OPL, OL, and OP) and different parameter sets of $\{\epsilon_l, \epsilon_h\}$, i.e., {v,0.1}, {v,0.9}, {0.9,v}, ('v' is to note variable ϵ_l or ϵ_h). In general, it is observed that EE_l improves with the increase of ϵ_l and ϵ_h

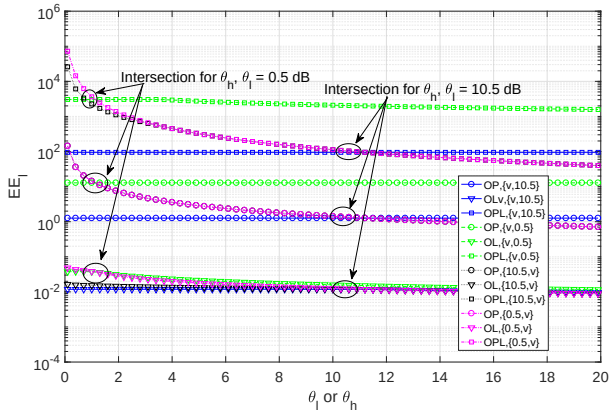

Fig. 3. LPS's EE versus SIR. Parameters: $P_{l,h} = 25$dBm, $\epsilon_{l,h}$=0.3,$R_{l,h}$=2m,k_t=1, $\lambda_{l,h}$=0.5e-4.

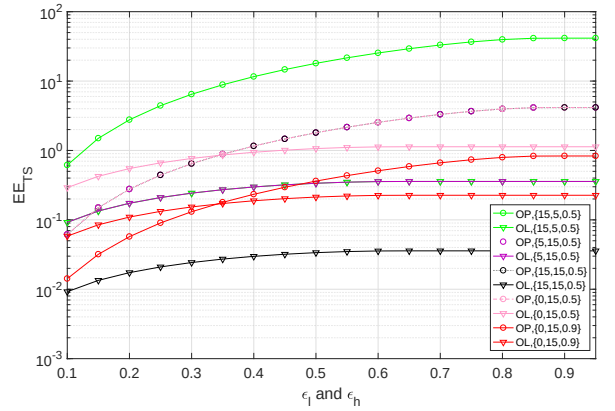

Fig. 4. Combined LPS and HPS EE versus tolerance threshold. Parameters: $R_{l,h}$=4m,$\epsilon_{l,h}$ = 0.2,$\theta_{l,h}$=4dB,k_t=1,$\lambda_{l,h}$=1e-4.

(since the feasibility region becomes larger), except for OP with $\epsilon_l = 0.9$ where both constraints are always inactive. Also, as expected OPL outperforms both OL and OP schemes. Under OL scheme, we note an increase in EE$_l$ up-to a certain point, (a) or (b), then the performance saturates. This is because the constraint related to ϵ_h is active at (a), whereas, the one related to ϵ_l becomes inactive and the optimal λ_l has been achieved at (b). Point (a) occurred before (b) because of the difference in constraint tolerance, $\epsilon_h = 0.1, 0.9$, respectively. Same behavior is noted for OP scheme, as lower power constraint is inactive after point (c), where it was active before this point. As for point (d) on scheme OPL, the node density constraint related to ϵ_h is active for curve {v,0.1} (hence the optimal λ_l is constant). Yet, improvement could be made for both ({v,0.1} & {v,0.9}) curves because of the impact of increasing ϵ_l on power lower bound, P_s^-. The saturation after point (e) on both curves ({v,0.1} & {v,0.9}) occurs because there is no impact of ϵ_l on the optimal power. Similar behavior is inferred for the {0.1,v} curve at (f).

Figure 3 evaluates the EE$_l$ versus θ_l or θ_h, noted in the legend as $\{\theta_h, \theta_l\}$ and set as {v,10.5}, {v,0.5}, {10.5,v},{0.5,v} ('v' is to note variable θ_l or θ_h). It is clear that EE$_l$ is decreasing with θ, while variable θ_l has higher effect on the variance of EE$_l$, in compared to variable θ_h. Note that {v,10.5} intersects with {10.5,v} around $\theta_l = 10.5$ for OPL, OL, and OP curves. Hence, to have relatively high EE$_l$ (in compared to EE$_h$) it is preferred to set $\theta_l < \theta_h$. As expected, it is observed that OPL scheme outperforms both OP and OL for all values of θ_l and θ_h.

Figure 4 evaluates EE, EE$_{TS}$, against variable ϵ_l and ϵ_h, for both OL and OP schemes, under several variation of power and weight sets, i.e., $\{P_l, P_h, \alpha_h\} = \{15, 5, 0.5\}, \{5, 15, 0.5\}, \{15, 15, 0.5\}, \{0, 15, 0.5\}, \{0, 15, 0.9\}$. Note that Unlike Fig. 2, both ϵ_l and ϵ_h change similarly, as an x-axis. A general observation for both schemes is that if the P_l/P_h ratio is high or low ($>> 1$ or $<< 1$), then the dominating EE is the one corresponding to the lower power (if P_l/P_h is low it follows that EE$_l$ is dominating). However, if P_l/P_h is close to one, then the dominating EE is the one with higher weight, α_l or α_h. Also, the OP performance for different curves of $\{5, 15, 0.5\}, \{15, 15, 0.5\}, \{0, 15, 0.5\}$ is the same because we model the denominator of $\mathcal{E}_h$ and $\mathcal{E}_l$ to be $k_t P_h$ and $k_t P_l = k_t \zeta P_h$, respectively, (fixing P_h while optimizing the ratio ζ). Hence, the critical parameters are the constant P_h and α_h. We observe that for OL curves decreasing the ratio P_l/P_h will shift the intersection point of the curves OL and OP to the right, i.e., it requires higher tolerance, ϵ_l and ϵ_h, for OP to outperform OL.

VI. Conclusion

In this work, we tackled a cognitive radio environment where multiple LP and HP users coexist in the same area. We maximize the energy efficiency of each system by proposing two schemes. The strict quasi-concave and pseudo-concave structures of the addressed problems have been proved. We further construct a multi-objective optimization problem to maximize both HP and LP energy efficiency performance. This multi-objective problem is solved via linear combination scheme and product combination scheme. An iterative alternating algorithm is proposed to guarantee a global optimal solution for the multi-objective problem. Selected numerical results have shown the improvement of jointly optimizing the spatial density and transmission power in comparison to individual optimization. The improvement reaches up to 11 dB for certain parameters.

Appendix A
Proof of Lemma 1

In order to proof Lemma 1 it is necessary to show that the objective function $\mathcal{E}_l$ in (5) is concave or pseudo-concave with respect to P_n. In [17], it is shown that to show that a function is pseudo-concave it is enough to verify its quasi-concavity and show that it has a local maximum. Satisfying the pseudo-concavity structure enables us to utilize the Lagrangian theorem and the KKT conditions to obtained the optimal solution [17]. To verify this structure we divide $\mathcal{E}_l$ into numerator and denumerator, i.e., $\mathcal{E}_l = \frac{\mathcal{E}_{se}}{\mathcal{E}_{sd}}$, where $\mathcal{E}_{se} = \lambda_l \exp\left(-\eta_l'\left(\lambda_l + \lambda_h \frac{P_h^{\frac{2}{\alpha}}}{P_n}\right)\right)$ and $\mathcal{E}_{sd} = k_t P_n^{\frac{\alpha}{2}}$. It is easy to verify that $\mathcal{E}_{se}$ is strictly concave and $\mathcal{E}_{sd}$ is strictly convex with respect to P_n, given $\alpha > 2$ (which is a valid assumption this framework). These structures of $\mathcal{E}_{se}$ and $\mathcal{E}_{sd}$ are utilized in the following proof of strict quasi-concavity

structure of $\mathcal{E}_l$. We first define a quasi-concave function as follows,

Definition A function $f(x)$ is strict quasi-concave if

$$f(\lambda x^{(1)} + \lambda x^{(2)}) > \min\{f(x^{(1)}), f(x^{(2)})\}. \tag{37}$$

Then, the strict quasi-concavity proof is provided as follows,

$$\mathcal{E}_{se}\left(\lambda P_l^{(1)} + (1-\lambda)P_l^{(2)}\right) \tag{38a}$$
$$> \lambda\mathcal{E}_{se}\left(P_l^{(1)}\right) + (1-\lambda)\mathcal{E}_{se}\left(P_l^{(2)}\right) \tag{38b}$$
$$> \lambda\mathcal{E}_{sd}\left(P_l^{(1)}\right)\frac{\mathcal{E}_{se}\left(P_l^{(2)}\right)}{\mathcal{E}_{sd}\left(P_l^{(2)}\right)} + (1-\lambda)\mathcal{E}_{se}\left(P_l^{(2)}\right) \tag{38c}$$
$$> \frac{\mathcal{E}_{se}\left(P_l^{(2)}\right)}{\mathcal{E}_{sd}\left(P_l^{(2)}\right)}\left[\mathcal{E}_{sd}\left(\lambda P_l^{(1)} + (1-\lambda)P_l^{(2)}\right)\right] \tag{38d}$$
$$\implies \mathcal{E}_l\left(\lambda P_l^{(1)} + (1-\lambda)P_l^{(2)}\right) \geq \mathcal{E}_l\left(P_l^{(2)}\right), \tag{38e}$$

where (38c) results by assuming that $\mathcal{E}_l(P_l^{(2)}) < \mathcal{E}_l\left(P_l^{(1)}\right)$, (38d) is valid because of the strict convex property of $\mathcal{E}_{sd}(P_l)$. This proof verifies the strict quasi-concave property of $\mathcal{E}_l$ with respect to P_l.

After verifying the quasi-concavity structure of $\mathcal{E}_l$, we now need to show that $\mathcal{E}_l$ has a local maximum. It is clear that $\nabla\mathcal{E}_l(P_l^*) = 0$ iff $\nabla\mathcal{E}_{se}(P_l^*)\mathcal{E}_{sd}(P_l^*) - \mathcal{E}_{se}(P_l^*)\nabla\mathcal{E}_{sd}(P_l^*) = 0$. Then, $\nabla\mathcal{E}_{se}(P_l^*) = \mathcal{E}_l(P_l^*)\nabla\mathcal{E}_{sd}(P_l^*)$. Utilizing the properties of $\mathcal{E}_{se}$ function,

$$\mathcal{E}_{se}(P_l) < \mathcal{E}_{se}(P_l^*) + \nabla\mathcal{E}_{se}(P_l^*)(P_l - P_l^*) \tag{39a}$$
$$= \mathcal{E}_{se}(P_l^*) + \mathcal{E}_l(P_l^*)\nabla\mathcal{E}_{sd}(P_l^*)(P_l - P_l^*) \tag{39b}$$
$$< \mathcal{E}_{se}(P_l^*) + \mathcal{E}_l(P_l^*)(\mathcal{E}_{sd}(P_l) - \mathcal{E}_{sd}(P_l^*)) \tag{39c}$$
$$= \mathcal{E}_{se}(P_l^*) + \mathcal{E}_l(P_l^*)\mathcal{E}_{sd}(P_l) - \mathcal{E}_{se}(P_l^*) \tag{39d}$$
$$\implies \frac{\mathcal{E}_{se}(P_l)}{\mathcal{E}_{sd}(P_l)} \geq \mathcal{E}_l(P_l^*), \tag{39e}$$

where (39a) follows from the strict concave property of $\mathcal{E}_{se}$ and (39c) is due to the strict convex structure of $\mathcal{E}_{sd}(P_l)$.

Showing that $\mathcal{E}_l$ has a maximum point and it is quasi-concave, then it is clear that $\mathcal{E}_l$ is strict pseudo-concave. Therefore, the Lagrangian theory and KKT can be utilized to find the optimal solution [17], as provided by Lemma 1.

Appendix B
Proof of Lemma 2

To verify Lemma 2 we use similar approach as in Appendix B, i.e., proving the pseudo-concavity structure of the problem with respect to to λ_l. To show the pseudo-concavity structure of $\mathcal{E}_l$ we utilize the first order definition, as in [17].

Definition A function $f(x)$ is pseudo-concave if it is increasing then decreasing on x with a local maximum.

The first derivative of $\mathcal{E}_l$ is expressed as follows,

$$\frac{\partial\mathcal{E}_l}{\partial\lambda_l} = (k_t P_l)^{-1} e^{-\eta_s'\left(\lambda_l + \lambda_h\left(\frac{P_h}{P_l}\right)^{\frac{1}{\alpha}}\right)}\left[1 - \lambda_l\eta_l'\right] \tag{40}$$

From the first derivative we note that $\mathcal{E}_l$ is increasing for $\lambda_l < \frac{1}{\eta_s'}$ and decreasing for $\lambda_l > \frac{1}{\eta_s'}$, and it has a local maximum at $\lambda_l = \frac{1}{\eta_s'}$. Thus, it is clear that $\mathcal{E}_l$ is a strict pseudo-concave on λ_l. Hence Lemma 2 can be verified by satisfying the Lagrangian theorem and KKT conditions.

Appendix C
Proof of Theorem 1

In order to prove Theorem 1 it is sufficient to show that problem (17) is pseudo-concave with quasi-concave constraints. The constraints are clearly quasi-concave. To show that the objective function is jointly pseudo-concave, we utilize the fact that a jointly log-concave function is a jointly pseudo-concave with respect to to all variable [18]. Therefore, we now focus on proving the log-concavity characteristic of (17a). The logarithm of function (17a) is expressed as follows,

$$\log(\mathcal{E}_l) = \log(\lambda_l) - \eta_l'\lambda_l - \eta_l'\lambda_h\zeta_s - \log(k_t P_h) + \frac{\alpha}{2}\log(\zeta_s) \tag{41}$$

We can show the joint concavity of $log(\mathcal{E}_l)$ via two ways, we can either prove the negative semi-definite property of $log(\mathcal{E}_l)$ or we can express $log(\mathcal{E}_l)$ as a sum of two function and prove the concavity of each one as follows. Let $log(\mathcal{E}_l) = g_1(\lambda_l) + g_2(\zeta_s)$, where $g_1(\lambda_l) = \log(\lambda_l) - \eta_l'\lambda_l$ and $g_2(\zeta_s) = -\eta_l'\lambda_h\zeta_s - \log(k_t P_h) + \frac{\alpha}{2}\log(\zeta_s)$. It is straight forward to show that $g_1(\lambda_l)$ is concave with respect to λ_l and $g_2\zeta_s$ is concave with respect to ζ_s. We know from optimization theory that a sum of concave function result in a joint concave function. Therefore, $log(\mathcal{E}_l)$ is jointly concave function with respect to to both λ_l and ζ_s. Hence, $\mathcal{E}_l$ is jointly pseudo-concave function and problem (17) can be solved by satisfying the Lagrangian theory and KKT conditions.

Form geometric optimization theory, we know that transforming the objective function with a monotone function results in equivalent problem, thus, equivalent solution [16]. We then derive the associated Lagrangian function with $\log(\mathcal{E}_l)$ and the corresponding constraints as follows,

$$\begin{aligned}\mathcal{L}_{sr} = &\log(\lambda_l) - \eta_s'\lambda_l - \eta_s'\lambda_h\zeta_s - \log(k_t P_h) + \frac{\alpha}{2}\log(\zeta_s)\\ &- \lambda_1\left(\lambda_l + \lambda_h\zeta_s\frac{\log(1-\epsilon_s)}{\eta_s'}\right)\\ &- \lambda_2\left(\lambda_l + \zeta_s\left(\lambda_h + \frac{\log(1-\epsilon_h)}{\eta_p'}\right)\right)\end{aligned} \tag{42}$$

The optimal expressions in (18) and (19) are found by obtaining the zeros of $\frac{\partial\mathcal{L}_{sr}}{\partial\zeta_s} = 0$ and $\frac{\partial\mathcal{L}_{sr}}{\partial\lambda_l} = 0$, respectively.

Appendix D
Proof of Proposition 1

To proof Proposition 1, we must show that utilizing the generalized theory of convex optimization, i.e., Lagrangian function and KKT conditions, applies to problem (21). Hence, in here, we proof the strict quasi-concavity of $\mathcal{E}_{TS}$ in P_n and P_{np}. The necessity of proving the strictness is because in Alg. 1 we will utilize this property to propose an iterative global solution for problem 20. The proof of strict quasi-concavity of $\mathcal{E}_{TS}$ with respect to P_n can be derived by straight forward

steps from Appendix A. Whereas, the strict quasi-concavity of $\mathcal{E}_{TS}$ with respect to P_{np} is easily observed since the function is strictly decreasing on P_{np}. To derive the expression in (23), we must observe that maximizing $\mathcal{E}_{TS}$ with respect to P_n is equivalent to the following problem,

$$\max_{(P_s^-)^{\frac{2}{\alpha}} \leq P_n \leq (P_s^+)^{\frac{2}{\alpha}}} \quad \alpha_l \frac{\lambda_l \exp\left(-\eta_l'\left(\lambda_l + \lambda_h \frac{P_h^{\frac{2}{\alpha}}}{P_n}\right)\right)}{k_t P_n^{\frac{\alpha}{2}}} \tag{43a}$$

$$\text{s.t.} \qquad P_n = P_{np} \tag{43b}$$

Note that the solution of this problem is different than that of (9) because we including the equality constraint $P_n = P_{np}$. We then use the transformation on the objective function in (43a) using monotone increasing function, i.e., $\log(.)$. The corresponding Lagrangian function of problem (43) is expressed as follows,

$$\mathfrak{L} = \log\left(\frac{\alpha_s \lambda_l}{k_t}\right) - \eta_s' \lambda_l - \eta_s' \lambda_h \frac{P_u}{P_n} - \frac{\alpha}{2}\log\left(P_n\right) + \mu\left[P_n - P_{np}\right], \tag{44}$$

where $P_u = P_h^{\frac{2}{\alpha}}$. Taking the derivative of the Lagrangian function in (44) and finding its zeros results in the following,

$$2\mu P_n^2 - \alpha P_n + 2\eta_s' \lambda_h P_u = 0. \tag{45}$$

Hence, the expression in (23) is easily obtained by solving (45).

We then derive the expression in (25), by observing that maximizing $\mathcal{E}_{TS}$ with respect to P_{np} is equivalent to the following problem,

$$\max_{(P_s^-)^{\frac{2}{\alpha}} \leq P_{np} \leq (P_s^+)^{\frac{2}{\alpha}}} \quad \alpha_h \frac{\alpha_h \lambda_h \exp\left(-\eta_h'\left(\lambda_h + \frac{\lambda_l P_{np}}{P_h^{\frac{2}{\alpha}}}\right)\right)}{(k_t P_h)} \tag{46a}$$

$$\text{s.t.} \qquad P_n = P_{np}. \tag{46b}$$

We then formulate the Lagrangian function of (46), devise its first derivative and find its zeros as follows,

$$\frac{-\alpha_p \lambda_h \eta_p' \lambda_l e^{-\eta_p' \lambda_h}}{k_t P_u^{\frac{\alpha}{2}}} \exp\frac{-\eta_p' \lambda_l P_{np}}{P_u} + \mu = 0. \tag{47}$$

Solving (47) leads to the exact solution in (25).

Appendix E
Proof of Proposition 2

To verify Proposition 2 we show that $\mathcal{E}_{TS}$ is strictly quasi-concave with respect to λ_l. This enables us to use the principles of generalized convexity theory, Lagrangian theory and KKT conditions, in addition to guarantee convergence of the alternating optimization algorithm proposed in Algorithm 1.

Let us use $\mathcal{E}_{TS} \uparrow$ to note that $\mathcal{E}_{TS}$ is increasing and $\mathcal{E}_{TS} \downarrow$ to note that $\mathcal{E}_{TS}$ is decreasing. The first derivative of $\mathcal{E}_{TS}$ with respect to λ_l can be expressed as follows,

$$\frac{\partial \mathcal{E}_{TS}}{\partial \lambda_l} = \mathcal{E}_{TS}^{(\lambda_l)} = \left[a - ab\lambda_l - cde^{-(d-b)\lambda_l}\right] e^{-b\lambda_l} \tag{48}$$

where a, b, c, and d are positive constants with respect to λ_l. Let us analyze the behavior of $\mathcal{E}_{TS}$ as $\lambda_l \to \infty$, it is clear that

$$\lim_{\lambda_l \to \infty} \mathcal{E}_{TS}^{(\lambda_l)} \underset{\mathcal{E}_{TS}\downarrow}{\overset{\mathcal{E}_{TS}\uparrow}{\gtrless}} 0 \Leftrightarrow \lim_{\lambda_l \to \infty} a - ab\lambda_l - cde^{-(d-b)\lambda_l} \underset{\mathcal{E}_{TS}\downarrow}{\overset{\mathcal{E}_{TS}\uparrow}{\gtrless}} 0 = -\infty \overset{\mathcal{E}_{TS}\downarrow}{<} 0 \tag{49}$$

This means that $\mathcal{E}_{TS}$ is decreasing at large λ_l. We now analyze the behavior of $\mathcal{E}_{TS}$ as $\lambda_l \to 0$,

$$\lim_{\lambda_l \to 0} \mathcal{E}_{TS}^{(\lambda_l)} \underset{\mathcal{E}_{TS}\downarrow}{\overset{\mathcal{E}_{TS}\uparrow}{\gtrless}} 0 \Leftrightarrow \lim_{\lambda_l \to 0} a - ab\lambda_l - cde^{-(d-b)\lambda_l} \underset{\mathcal{E}_{TS}\downarrow}{\overset{\mathcal{E}_{TS}\uparrow}{\gtrless}} 0 = a - cd \underset{\mathcal{E}_{TS}\downarrow}{\overset{\mathcal{E}_{TS}\uparrow}{\gtrless}} 0 \tag{50}$$

It is necessary to verify the number of local stationary points (maxima or minima) for $\mathcal{E}_{TS}$. This is can be easily identified as the number of zeros of (48). We know that (48) has only one zero, which is found in (29). This means that this zero lies in the positive domain of λ_l, i.e., $\lambda_l^* \in [0, \infty)$, or the zero lies in the negative domain, i.e., $\lambda_l^* \in (-\infty, 0]$. We conclude from the first case that $\mathcal{E}_{TS}$ is strictly pseudo-concave with respect to λ_l. Since, the negative values of λ_l are not in the domain of this problem, then $\mathcal{E}_{TS}$ is strict quasi-concave with respect to λ_l, hence there is a unique maximum point of $\mathcal{E}_{TS}$ This conclude the proof of Proposition 2.

Appendix F
Proof of Theorem 2

To proof Theorem we need to satisfies the conditions of the findings in [19]. Grippo and Sciandrone, in [19], verified that using Gauss-Seidel method to optimize over several variable guarantee a global optimal solution without the necessity of proving joint concavity/convexity structure. The condition which must be met is to prove that the targeted problem is strict quasi-concave with respect to to each individual variable. Therefore, to proof F, it is enough to verify the strict quasi-concave property of problem $\mathcal{E}_{TS}$ with respect to each variable P_n, P_{np}, P_u, P_{us}, λ_l, λ_{sp}. We have already proven the strict quasi-concave of P_n, P_{np}, and λ_l in Appendices D and E, respectively. In similar lines as in Appendices D and E we can prove the strict quasi-concave structure of $\mathcal{E}_{TS}$ with respect to P_u, P_{us}, and λ_h. This conclude the proof of Theorem 2.

References

[1] W. Ye, J. Heidemann, and D. Estrin, "Medium access control with coordinated adaptive sleeping for wireless sensor networks," *IEEE/ACM Transactions on Networking*, vol. 12, no. 3, pp. 493–506, June 2004.

[2] J. Wu, G. Wang, and Y. Zheng, "Energy efficiency and spectral efficiency tradeoff in Type-I ARQ systems," *IEEE Journal on Selected Areas in Communications*, vol. 32, no. 2, pp. 356–366, February 2014.

[3] A. Alabbasi, Z. Rezki, and B. Shihada, "Energy efficient resource allocation for cognitive radios: A generalized sensing analysis," *IEEE Transactions on Wireless Communications*, vol. 14, no. 5, pp. 2455–2469, May 2015.

[4] M. Haenggi, *Stochastic Geometry for Wireless Networks*. Cambridge University Press, 2012.

[5] J. Lee, S. Lim, J. Andrews, and D. Hong, "Achievable transmission capacity of secondary system in cognitive radio networks," in *IEEE International Conference on Communications (ICC), 2010*, May 2010, pp. 1–5.

[6] O. Galinina, S. Andreev, M. Gerasimenko, Y. Koucheryavy, N. Himayat, S.-P. Yeh, and S. Talwar, "Capturing spatial randomness of heterogeneous cellular/wlan deployments with dynamic traffic," *IEEE Journal on Selected Areas in Communications*, vol. 32, no. 6, pp. 1083–1099, June 2014.

[7] S. Weber, J. Andrews, and N. Jindal, "An overview of the transmission capacity of wireless networks," *IEEE Transactions on Communications*, vol. 58, no. 12, pp. 3593–3604, December 2010.

[8] J. Lee, J. Andrews, and D. Hong, "Spectrum-sharing transmission capacity with interference cancellation," *IEEE Transactions on Communications*, vol. 61, no. 1, pp. 76–86, January 2013.

[9] ——, "Spectrum-sharing transmission capacity," *IEEE Transactions on Wireless Communications*, vol. 10, no. 9, pp. 3053–3063, September 2011.

[10] T. Q. S. Quek, W. C. Cheung, and M. Kountouris, "Energy efficiency analysis of two-tier heterogeneous networks," in *Wireless Conference 2011 - Sustainable Wireless Technologies (European Wireless), 11th European*, April 2011, pp. 1–5.

[11] Y. Kwon and T. Hwang, "A game-theoretic approach for energy-efficient power control in spectrum sharing networks," in *2014 IEEE International Conference on Communications (ICC)*, June 2014, pp. 3493–3498.

[12] R. Hernandez-Aquino, S. A. R. Zaidi, D. McLernon, and M. Ghogho, "Energy efficiency analysis of two-tier mimo diversity schemes in poisson cellular networks," *IEEE Transactions on Communications*, vol. 63, no. 10, pp. 3898–3911, Oct 2015.

[13] H. H. Yang, G. Geraci, and T. Q. S. Quek, "Energy-efficient design of mimo heterogeneous networks with wireless backhaul," *IEEE Transactions on Wireless Communications*, vol. PP, no. 99, pp. 1–1, 2016.

[14] W. Nie, Z. Yi, F. Zheng, W. Zhang, and T. O'Farrell, "Hetnets with random dtx scheme: Local delay and energy efficiency," *IEEE Transactions on Vehicular Technology*, vol. PP, no. 99, pp. 1–1, 2015.

[15] M. Haenggi and R. K. Ganti, "Interference in large wireless networks," *Foundations and Trends in Networking*, vol. 3, no. 2, pp. 127–248, 2008. [Online]. Available: http://dx.doi.org/10.1561/1300000015

[16] S. Boyd and L. Vandenberghe, *Convex Optimization*, 2004.

[17] A. Cambini and L. Martein, *Generalized Convexity and Optimization: Theory and Applications*. Springer, 2008.

[18] K. P. and M. J., *Stochastic Linear Programming Models, Theory, and Computation*. Springer, 2011.

[19] L. Grippo and M. Sciandrone, "On the convergence of the block nonlinear Gauss-Seidel method under convex constraints," *Operations Research Letters*, vol. 26, no. 3, pp. 127 – 136, 2000.